Robust and optimal control analysis of sun seeker system

S. K. Jha*, A.K. Yadav[*], Prerna Gaur[*], J.R.P. Gupta[*], H. Parthsarathy[**]

[*]*Division of Instrumentation and Control Engineering, NSIT, Dwarka, New Delhi*
(email:jhask271@gmail.com, anilei007@gmail.com, prernagaur@yahoo.com, jrpg83@yahoo.com)
[**]*Division of Electronics and Communication Engineering, NSIT, Dwarka, New Delhi*
(email: harisignal@yahoo.com)

Abstract: The objective of this paper is to design the robust and optimal controller to control the attitude of sun seeker system (SSS) mounted on a space vehicle to extract maximum possible current by photo voltaic (PV) cells. PV cells which are employed to provide energy to the space vehicle generates maximum current when sun's rays are vertically incident over it. Hence sun seeker axis (SSA) position is continuously controlled to adjust the position of PV cells. Internal model controller (IMC) for robust and linear quadratic regulator (LQR) for optimal control is proposed. The result of proposed controller is compared with classical proportional integral derivative (PID) controller and pole placement technique (PPT) based controller.

Keywords: IMC, LQR, Optimal control, PID, PPT, Robust control, Renewable energy sources, Space vehicle, Sun-seeker system.

1. INTRODUCTION

In the light of the inevitability of burgeoning crisis of conventional energy resources, hunt for alternative renewable energy source is indispensable. In recent years increasing concern of environment and ecology has made the use of non-conventional energy sources obligatory for modern scientists and researchers. The exhaust emissions of the conventional internal combustion engine vehicles are the major source of urban pollution that causes the greenhouse effect, which in turn leads to global warming (Husain, 2011). On the other hand, photovoltaic (PV) cell and for that matter any other renewable energy sources (RESs) is need of the hour. Furthermore, RESs such as PV cell having no emissions are capable of tackling the pollution problem in an efficient way and may lead to the design of zero emissions vehicles (ZEVs) which eventually obviates the pollutant emission like carbon monoxide, hydrocarbon and nitrogen oxide etc. (Husain, 2011; Gevorkian, 2011; Ehsani *et al.,* 2011; Kiencke *et al.,* 2007; Yadav *et al.,* 2011).

In order to understand the subtlest and inscrutable aspect of this nature and environment, the space scientist world over are engaged to employ space vehicle for exploration works. Under the precarious and dwindling condition of fossil fuels, government world over is trying to use renewable energy sources in every walk of life. In light of this in the present work, photo voltaic (PV) cells are employed to provide the required energy to space vehicle. Since the current generated by each PV cell is proportional to illumination of the cell, light need to be precisely centered on the cells. Hence PV cells generate maximum current when sun's rays are vertically incident over it. The sun seeker system (SSS) is mounted on space vehicle to adjust the position of PV cells so that sun's light is precisely centered on it. The objective of sun seeker system is to manoeuvre its own attitude continuously so as to extract maximum possible current from photo voltaic cell to be instantly used by space vehicle. The implication of attitude control of SSS is nothing but to control the position of sun seeker axis (SSA) continuously to bring it in the direction of sun's ray. The benefit of sun seeker system is that it is designed and tested to endure all weather condition and up to 25% more power is generated as compared to permanently fixed or tilted system provided the SSS should be robustly and optimally controlled while tracking the sun. In order to extract maximum energy under erratic conditions and parametric uncertainties, study and design of robust and optimal controller has drawn the attention of many researchers in recent years (Kiencke *et al.,* 2007; Yadav *et al.,* 2011). The designed system is said to be robust if it remains insensitive to the presence of parametric uncertainties and optimal if response is faster and energy consumption is minimum.

In this paper the example of sun seeker system (SSS) is presented to precisely control its attitude so that it will track the sun with high accuracy and efficiency (Kuo *et al.,* 2003). Here we intend to control SSA of SSS mounted on space vehicle so that the efficiency of photovoltaic cell is maximum. In order that the SSS track the sun with high accuracy and efficiency, SSA should completely align with the solar axis. Therefore the main objective here is to minimize the error of alignment between these two axes to zero value. But due to relative movement between sun and the earth, solar axis changes its position continuously therefore only way out to get maximum current by PV cell is to somehow align the sun seeker axis (SSA) repeatedly in the direction of sun ray. For accomplishing this task the attitude of the SSS must be controlled by some sophisticated control mechanism so that the SSA may be realigned with the solar axis in order to generate maximum current by PV cell. Here for this purpose optimal and robust controller has been used to control the attitude in a robust and optimal manner

leveraging the robust and optimal features of the respective controller. So, whenever there is nonalignment between solar-axis and SSA due to relative movement between sun and earth, an error is generated and the same is sent to controllers and servo amplifiers which in turn will cause the motor to drive the system back into alignment minimizing the error to zero. Hence proper tuning of PID, LQR and IMC are done and most effective controller is identified for better performance of the SSS.

From the standpoint of environmental and ecological repercussions and burgeoning popularity of RESs in the market, bewildering variety of energy management system is devised. As pioneers of intelligent energy management in RESs some authors have proposed an extensive classification and overviews of state of the art control strategies. The conventional control methods such as PID (Mikles and Fikar, 2007; Skogestad and Postlethwaite, 2001) have been found not so adequate and many control problems have come up due to imprecise input output relation and unpredictable nature of parameter variation (Gopal, 2009; Kakilli *et al.,* 2009; Gollman *et al.,* 2009; Peterson, 2009; Kirk, 1970).

Next the state feedback control technique such as PPT and LQR controller of optimal control segment came up with beautiful features of the later one to improve dynamic as well as steady state performance (Mi *et al.,* 2005; Canale *et al.*, 2009; Amuthan *et al.,* 2009; Li and Deng, 2006; Hamedmouna and Lassad, 2007). Some parameters of SSS are not always constant and may vary due to erratic conditions through which the vehicle has to pass. The system not being immune and insensitive to parameter variations necessitates the design of robust controller for better performance of PV cells. The attitude control of SSS is mainly achieved by controlling the servo motor which in turn controls the SSA position of SSS so that its ability to track the sun light is greatly optimized. Another control scheme such as IMC for the robust control of the SSS is also introduced which gives better performance as compared to PID, PPT and in some respect to LQR under parametric variations (Li and Deng, 2006; Hamedmouna and Lassad, 2007; Malan *et al.,* 2004; Harnefors and Nee, 1998; Borrelli and Keviczky, 2008; Yadav and Gaur, 2013).

2. PROBLEM FORMULATION AND MODEL DESCRIPTION

The schematic diagram of SSS is given in fig.1 (a) and corresponding simplified block diagram is given in fig.2 (Kuo and Golnaraghi, 2003). The principal elements are two mall silicon PV cells A and B mounted behind a rectangular slit. PV cells are used as current sources and connected in opposite polarity to the input of an op-amp. Since the current generated in each of the PV cell is proportional to the illumination of the cell, an error signal will occur at the output of the amplifier when the light is not precisely centred on the cells. This error voltage, when fed to controller in conjunction with servo amplifier, will cause the motor to drive the system back into alignment i.e., solar axis and SSA coincides with each other.

In the present system, tracking the sun in only one plane is accomplished and the angle α between solar axis and SSA is to be minimized. The reference axis of the coordinate system of the SSS is taken to be along the fixed frame of DC motor and all rotations are measured with respect to this axis. The angle θ_r denotes the desired angular position of SSA (in the direction of solar axis) and angle θ_o denotes the angular position of sun seeker axis with respect to reference axis respectively. Fig.1 (b) depicts the coordinate system for angular position of solar axis, sun seeker axis, and reference axis respectively. Fig.1(c) shows the schematic diagram of error discriminator of SSS. A general control model for the sun seeker system is presented in detail in appendix-A.

The motor position is given by angle θ_m. The angular position of the output gear θ_o and the motor position θ_m are related in terms of gear ratio n as $\theta_o = \theta_m/n$. In this section a sun-seeker system is modelled in order to facilitate its attitude control optimally so that it may track the sun with high accuracy. The numerical values of the parameters used for analysis of SSS are given in table 1.

Table 1. Numerical values of SSS parameters.

Parameters	Notation	Value (SI unit)
Op-Amp Gain	R_f	10,000 ohm
Armature Resistance	R_a	6.25 ohm
Back EMF constant	K_b	0.0125 V/rad/sec
Torque constant	K_i	0.0125 N-m/A
Moment of inertia	J	10^{-6} kg-m^2
Error Discriminator constant	K_s	0.1 A/rad
Viscous Friction Coefficient	B	0
Gear Ratio	N	800
Servo Amplifier Gain	K	0.5 (nominal value)

The objective of the control system is to minimize the error $\alpha(\mathrm{t})$ between $\theta_r(t)$ and $\theta_o(t)$, to zero:

$$\alpha(\mathrm{t}) = \theta_r(t) - \theta_o(t) \tag{1}$$

When the SSA is aligned perfectly with the solar axis, $\alpha(\mathrm{t}) = 0$, and the current $i_a(t)$ and $i_b(t)$ of cell A and cell B are equal i.e. $i_a(t) = i_b(t) = I$, or $i_a(t) - i_b(t) = 0$. From the geometry of the sun ray and the photovoltaic cells shown in fig.1(c) of error discriminator, when the SSA is not aligned perfectly with the solar axis, $\alpha(\mathrm{t}) \neq 0$, and the current $i_a(t)$ and $i_b(t)$ of cell A and cell B are dependent on α(t) as follows.

$$oa = \frac{W}{2} + L\ tan\ \alpha(t)$$
$$ob = \frac{W}{2} - L\ tan\ \alpha(t)$$

where oa denotes the width of the sun ray that shines on cell A, and ob is the same on cell B, for a given $\alpha(t)$. Since the current $i_a(t)$ is proportional to oa, and $i_b(t)$ is proportional to ob, we have

$$i_a(t) = I + \frac{2LI}{W}\ tan\ \alpha(t)$$
$$i_b(t) = I - \frac{2LI}{W}\ tan\ \alpha(t)$$

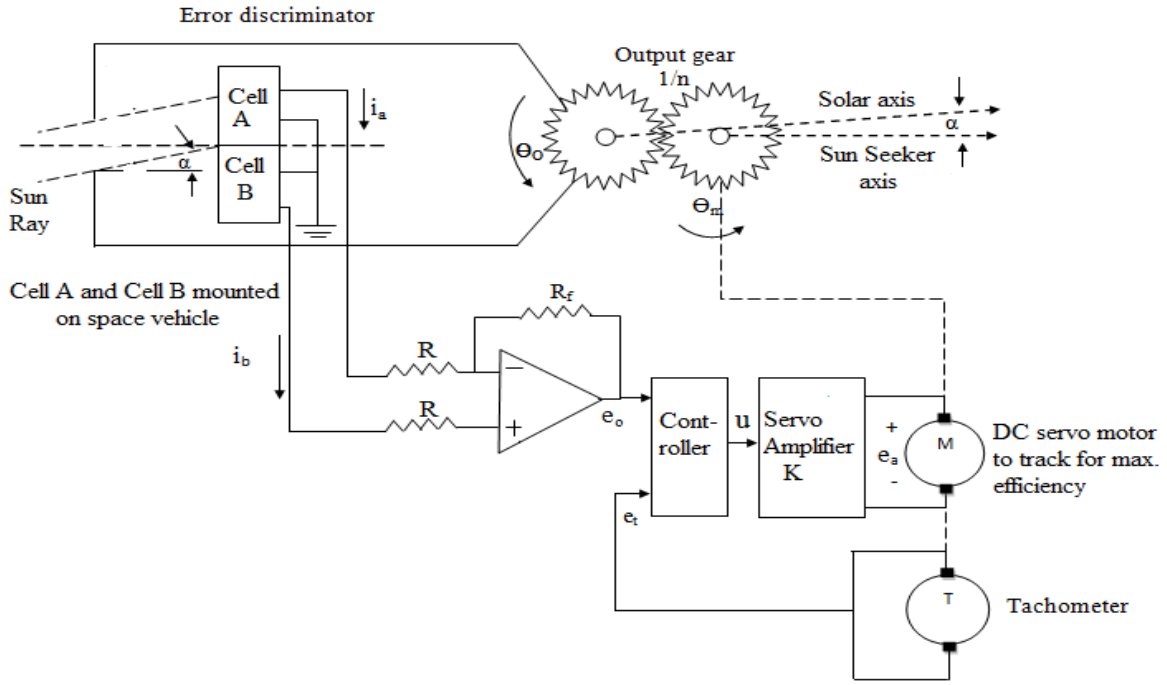

Fig. 1. (a) Schematic diagram of sun- seeker system.

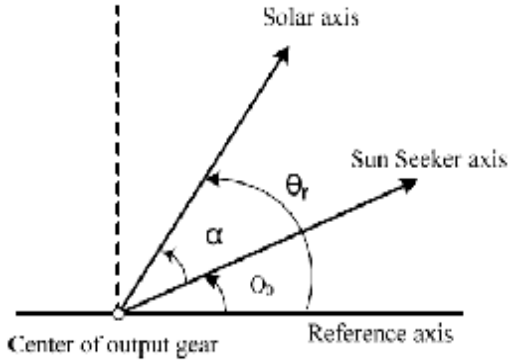

Fig. 1. (b) Coordinate system of sun seeker system.

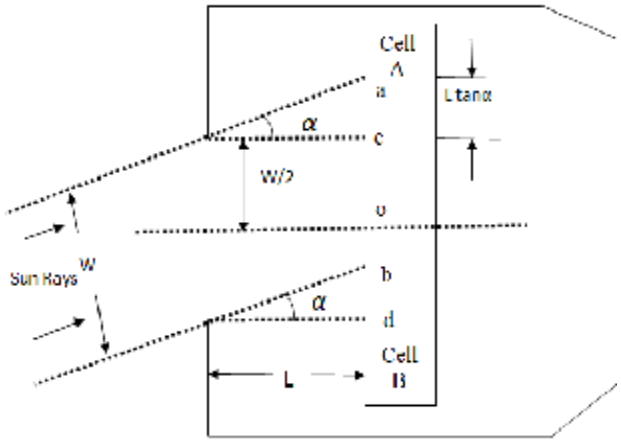

Fig. 1. (c) Schematic diagram of error discriminator of SSS.

Hence from above two equations for $i_a(t)$ and $i_b(t)$, we get the final equation for error discriminator as

$i_a(t) - i_b(t) = \frac{4LI}{W}\ tan\ \alpha(t)$

or

$$i_a(t) - i_b(t) = K_s\alpha(t) \quad (2)$$

where $K_s = \frac{4LI}{W}$, is called the error discriminator constant.

The relation between output of op-amp and the currents $i_a(t)$ and $i_b(t)$ is

$$e_o(t) = -R_f[i_a(t) - i_b(t)] \quad (3)$$

The output of the servo amplifier is expressed as

$$e_a(t) = -K[e_0(t) - e_t(t)] = -Ke_s(t) \quad (4)$$

The output voltage of the tachometer et is related to the angular velocity of the motor through the tachometer constant Kt.

$$e_t(t) = K_t\omega_m(t) = K_t\dot{\theta}_m \quad (5)$$

The angular position of the output gear is related to the motor position through the gear ratio1/n, hence

$$\theta_o = \frac{1}{n}\theta_m \quad (6)$$

The DC motor is modelled as below

$$e_a(t) = R_a i_a(t) + e_b(t) \quad (7)$$

$$e_b(t) = K_b\omega_m(t) \quad (8)$$

$$T_m(t) = K_i i(t) \quad (9)$$

$$T_m(t) = J\frac{d\omega_m(t)}{dt} + B\omega_m(t) \quad (10)$$

After combining (1) to (10), the open loop transfer function (OLTF) of SSS in terms of associated parameters is represented as OLTF:

$$G_P(s) = \frac{\theta_0(s)}{A(s)} = \frac{K_s R_f K_i K/n}{R_a Js^2 + K_i K_b s} \quad (11)$$

where $\theta_0(s)$ is SSA position and $A(s)$ is the Laplace transform of error signal $\alpha(t)$.

Putting the values from the table 1 in (11) we get OLTF:

$$G_P(s) = \frac{\theta_0(s)}{A(s)} = \frac{2500\,K}{s^2+25s} \quad (12)$$

The corresponding state space representation of sun seeker system for K=0.5 (nominal value) is given as

$$A = \begin{bmatrix} 0 & 1 \\ 0 & -25 \end{bmatrix}, B = \begin{bmatrix} 0 \\ 1250 \end{bmatrix}, C = [1\ 0], \quad (13)$$

where the matrix A, B, and C represents the system matrix, input matrix, and output matrix respectively.

In order to see the relative effectiveness of different controllers for the desired SSA position, here PID, PPT, IMC and LQR controllers are taken into consideration.

3. PID CONTROL

PID controllers are widely used in industrial control applications due to simple structures, comprehensible control algorithms and low cost. Fig. 3 shows the block diagram of PID control system. Fig.4 shows the simulink model of SSS with PID controller.

The transfer function of PID controller is given as

$$C(s) = K_P + \frac{K_i}{s} + K_d s = K_P\left(1 + \frac{1}{T_i s} + T_d s\right) \quad (14)$$

where Kp= Proportional Gain, Ki= Integral Gain, Ti= Reset Time = Kp / Ki, Kd = Derivative gain, Td= Rate time or derivative time = Kd /KP. Fig.4 shows the simulink model of SSS with PID controller. Here the set value (SV) is taken as the summation of step and ramp signals.

4. MODERN CONTROL TECHNIQUES

Here mainly two state space design methods, pole placement technique (PPT) and linear quadratic regulator (LQR) based techniques are considered. In pole placement design all closed loop poles are placed at desired locations.

4.1 State Feedback Control using PPT

Consider the linear time invariant (LTI) system with nth – order state differential equation

$$\dot{x}(t) = Ax(t) + Bu(t) \quad (15)$$

In the state feedback design, the control signal input u is realized as linear combinations of all the states, that is

$$u(t) = -k_1x_1(t) - k_2x_2(t) - \cdots k_nx_n(t)$$
$$= -kx(t) \quad (16)$$
$$k = [k_1k_2 \ldots . k_n] \quad (17)$$

k is a constant state feedback gain matrix.

The closed loop system is described by the state differential equation

$$\dot{x}(t) = (A - Bk)x(t) \quad (18)$$

The characteristics equation of the closed loop system is given as

$$|sI - (A - Bk)| = 0 \quad (19)$$

The desired characteristics equation is

$$(s - p_1)(s - p_2) \ldots \ldots \ldots (s - p_n) = 0 \quad (20)$$

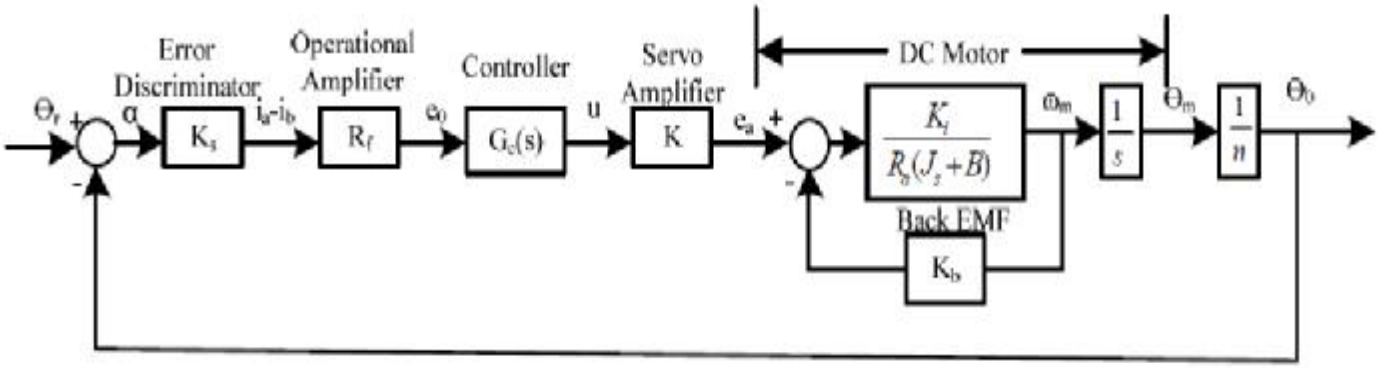

Fig. 2. Block diagram of sun seeker system.

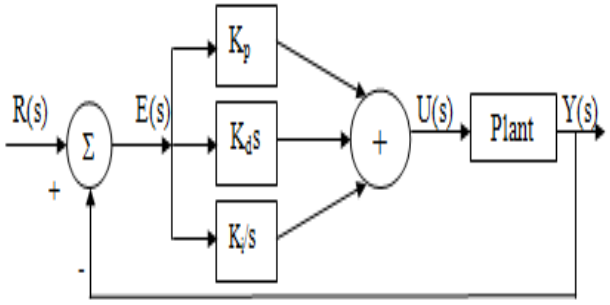

Fig. 3. Block diagram PID Control system.

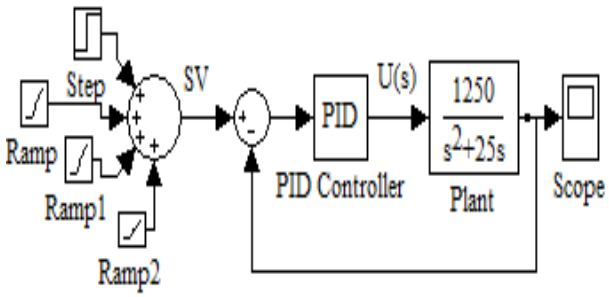

Fig. 4. Simulink model of plant with PID controller.

where $p_1, p_2, \ldots p_n$ are desired location of closed loop poles. The selection of desired closed loop poles requires a proper balance of settling time, rise time, bandwidth, and overshoot etc. The values of k are obtained by equating (19) and (20). Fig.5 shows the simulink model of State feedback controller via PPT.

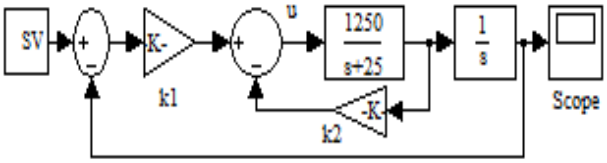

Fig. 5. Simulink model for PPT and LQR.

4.2 Linear Quadratic Regulator

Here an important class of optimal control problems known as linear regulator problem has been considered. Any problems having linear plant dynamics and quadratic performance criteria are referred to as linear regulator problem (Yadav et al., 2011; Kirk, 1970). The process i.e. SSS to be controlled is described by the state equations

$$\dot{x}(t) = A(t)x(t) + B(t)u(t) \tag{21}$$

Here the problem is to find an admissible control u* that causes the above process to follow an admissible trajectory $x*$ that minimizes the performance measure J of (22), which in turn will minimize the angle α between solar axis and vehicle axis.

$$J = \frac{1}{2}x^T(t_f)Sx(t_f) + \int_{t_0}^{t_f}\frac{1}{2}[x^TQx + u^TRu]dt \tag{22}$$

S and Q are real symmetric positive semi definite matrices; R is real symmetric positive definite matrix.

We can get the state equation, costate equation, and other important equation by defining the Hamiltonian as

$$H(x(t),u(t),\lambda(t),t) \triangleq g(x(t),u(t),t) + \lambda^T(t)[a(x(t),u(t),t)] \tag{23}$$

Using this notation, the necessary conditions can be written as follows:

$$\dot{x}^*(t) = \frac{\partial H}{\partial \lambda}(x^*(t),u^*(t),\lambda^*(t),t) \tag{24.a}$$

$$\dot{\lambda}^*(t) = -\frac{\partial H}{\partial x}(x^*(t),u^*(t),\lambda^*(t),t) \tag{24.b}$$

$$0 = \frac{\partial H}{\partial u}(x^*(t),u^*(t),\lambda^*(t),t) \tag{24.c}$$

and

$$\left[\frac{\partial h}{\partial x}(x^*(t_f),t_f) - \lambda^*(t_f)\right]^T \delta x_f + \left[H(x^*(t_f),u^*(t_f),\lambda^*(t_f),t_f) + \frac{\partial h}{\partial t}(x^*(t_f),t_f)\right]\delta t_f = 0 \tag{25}$$

Here from the performance measure (22) the Hamiltonian is

$$H[x(t),u(t),\lambda(t),t] = \frac{1}{2}x^TQx + \frac{1}{2}u^TRu + \lambda^TAx + \lambda^TBu \tag{26}$$

Using the equation (24) through (25)

$$\frac{\partial H}{\partial u} = 0 = R(t)u(t) + B^T(t)\lambda(t) \tag{27}$$

$$\frac{\partial H}{\partial x} = -\dot{\lambda} = Q(t)x(t) + A^T(t)\lambda(t) \tag{28}$$

with the terminal condition

$$\lambda(t_f) = \frac{\partial h}{\partial x(t_f)} = Sx(t_f) \tag{29}$$

Thus it is required that

$$u(t) = -R^{-1}(t)B^T(t)\lambda(t) \tag{30}$$

And it is inquired whether this may be converted to a closed-loop control by assuming that the solution for the adjoint is similar to (29)

$$\lambda(t) = P(t)x(t) \tag{31}$$

A closed control form is obtained from (30) and (31)

$$u(t) = -R^{-1}(t)B^T(t)\lambda(t) = -R^{-1}(t)B^T(t)P(t)x(t) \tag{32}$$

or

$$u(t) = -k(t)x(t) \tag{33}$$

where

$$k(t) = -R^{-1}(t)B^T(t)P(t) \tag{34}$$

This indicates that the optimal control law is a linear time varying function of the system states. Equation (33) gives the final optimal control law. The matrix $P(t)$ may be obtained by solving the matrix Riccati equation for finite duration. In order to arrive at eq. (34), where the feedback gain matrix is time varying, linear time variant system (21) is taken for finite duration. In the appendix-B, Kalman's modified matrix Riccati equation for a process of infinite duration has been derived where Kalman has shown that - if a few hypotheses ($S = 0$ and the matrix A, B, Q and R are constants) are satisfied then the matrix $P(t)$ will become a constant matrix P for an interval of infinite duration i.e. if $t_f \to \infty$. Hence from eq. (34) feedback gain matrix $k(t)$ will become constant feedback gain matrix k. Details of the derivation of Riccati equation for finite and infinite duration are explained in appendix B (Gopal, 2009; Kirk, 1970).

5. INTERNAL MODEL CONTROL

In this section the SSS under parametric uncertainties is controlled by internal model control which makes it robust and insensitive to parameter variation. The IMC consist mainly of the controller and system model (Mikles and Fikar, 2007; Hamedmouna and Lassad, 2007; Borrelli and Keviczky, 2008). The block diagram of IMC structure is given by fig.6.

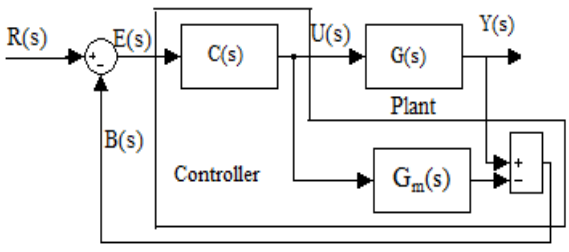

Fig. 6. Block diagram of IMC.

From fig.6

$$Y(s) = G(s)U(s) \tag{35}$$

$$B(s) = Y(s) - G_m(s)U(s) \tag{36}$$

$$U(s) = C(s)(R(s) - B(s)) \quad (37)$$

From (35) to (37)

$$Y(s) = \frac{G(s)C(s)R(s)}{1+C(s)(G(s)-G_m(s))} \quad (38)$$

The condition for perfect set point tracking is obtained if $G_m(s) = G(s)$ and $C(s)=1/G(s)$. If $G(s)$ is strictly proper, then its inverse model (1/G(s)) becomes improper. Hence in order to make a proper transfer function one filter is incorporated as a part of controller. The new controller is now defined as

$$Q(s) \triangleq \frac{1}{(\mu s+1)^n} G(s)^{-1} \quad (39)$$

Here n is suitably taken to make C(s) proper. The filter parameter μ influences the speed of response. Fig.7 shows the simulink model of IMC.

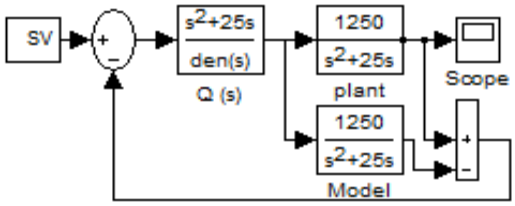

Fig. 7. Simulink model of IMC.

6. SIMULATION RESULTS AND DISCUSSION

In this section the results obtained from the open loop system without controller and closed loop system with various controllers are presented. The response of the system with controllers such as PID, PPT, Optimal LQR, and IMC are presented and compared for different values of servo amplifier gain K. Fig. 8 shows the open loop step response of sun seeker (SS) axis position with respect to time for different values of K which shows that the open loop system is unstable.

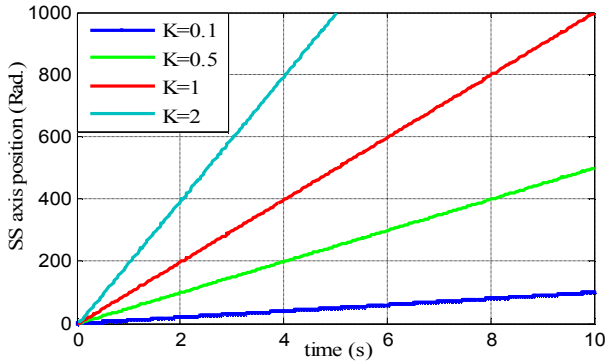

Fig. 8. Open loop step response.

Fig. 9a gives the response with P, PI and PID controller whose gains are tuned using Ziegler-Nichols (ZN) tuning method. The values of gains for P controller is $K_P = 0.84$ and for PI controller these are $K_P = 0.756$ and $K_I = 6.52$. The gains for PID controllers are given in table 2. It is observed from fig. 9a that steady state error (Ess) for P controller is larger in comparison to PI and PID, whereas for PI, overshoot is larger in comparison to P and PID. Therefore PID controller has been selected from the standpoint of both transient and steady state response. Fig. 9b shows the response of PID Controller only for nominal value of K = 0.5. Here PID controller is tuned using Hand-tuning rule (Amuthan et *al.*, 2009), Integral Time of Absolute Error (ITAE) and Ziegler-Nichols (ZN) method. The corresponding values of controller parameters are given in table 2.

After comparing the responses corresponding to different tuning method with respect to the set value (SV), it is observed that hand tuning method gives better performance. Initially only nominal value of K is considered from fig.10 through fig.12 to compare the performance of controller. Next, from fig.13 through fig.16, parametric uncertainties in terms of various values of K are taken into consideration to adjudge the efficacy of robust IMC and optimal LQR controller over PPT and classical PID controller.

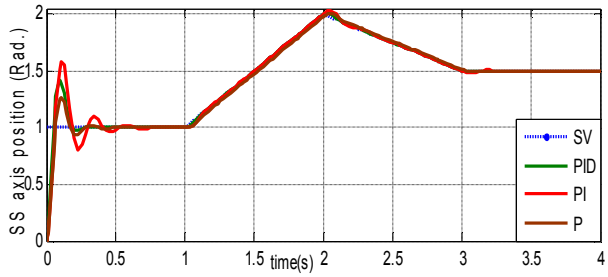

Fig. 9a Response with P, PI and PID Controller.

Table 2. PID Controller Parameters.

Tuning Method	K_P	K_I	K_D
Ziegler-Nichols	1.26	14.49	0.0175
ITAE	0.3872	2.7	0.001
Hand-tuning	7	1.8	0.05

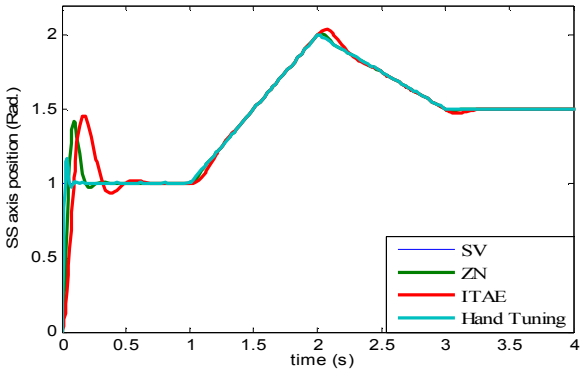

Fig. 9b. Response with PID Controller.

Fig.10 shows the response of sun seeker system (SSS) for PPT and LQR controllers for nominal value of K when the SV comprises sum of unit step and different ramp signal. In order to obtain a reasonable speed and damping in the response of designed system desired closed loop poles at $s = -13, -13$, are obtained after a number of trials so that the settling time is 0.3 to 0.5 sec. with negligible maximum overshoot. The corresponding desired characteristic equation for PPT is $s^2 + 26s + 169 = 0$.

In LQR the relative weights of matrix Q and R are taken as Q $=\begin{bmatrix}1 & 0\\ 0 & 0\end{bmatrix}$, R=10. The values of feedback gain constants k_1 and k_2 for PPT and LQR respectively are calculated by MATLAB

and given in table 3. Fig.10 shows the Optimal LQR response for SSS.

Table 3. State feedback gain parameters.

Techniques	k_1	k_2
PPT	0.1352	0.0008
LQR	0.3162	0.0101

Fig. 11 shows the IMC response of sun seeker (SS) axis position versus time with reference to SV taken to be same as the previous one and K is again nominal. For proper design of controller Q(s) of IMC, different value of filter parameters are taken as μ = 1, 0.5, 0.1, 0.01 for studying the effect of μ on the system performance. On decreasing the value of μ from 1 downward, settling and rise time is improved hence transient and steady state response is improved and system becomes faster.

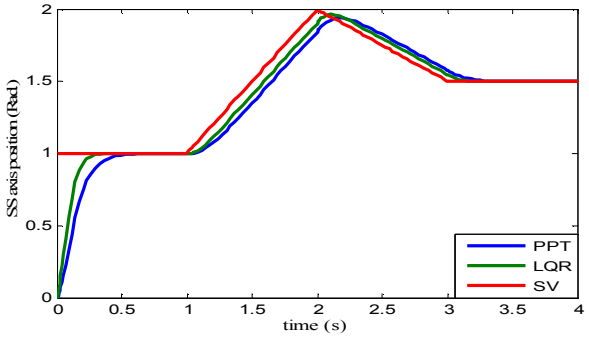

Fig. 10. PPT and Optimal LQR response .

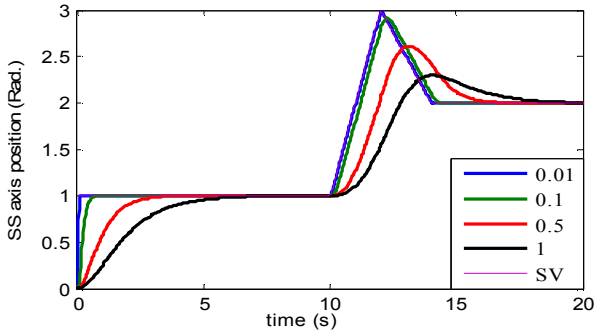

Fig .11. IMC response for different value of μ.

From fig. 11 it is obvious that μ=0.01 gives better performance with respect to other values of μ considered.

Hence in the consecutive discussion wherever IMC is involved, this best value of μ (= 0.01) only is taken into consideration. Smaller μ makes the response faster as is evident from fig. 11, which has direct implication with the bandwidth in frequency domain. As it is well known that the bandwidth is normally inversely proportional to the rise time hence if the system becomes faster for smaller μ it means bandwidth is higher**.** In this paper only time domain analysis has been considered. Fig.12 shows the unit step response of all controllers corresponding to nominal value of K and table 4 shows the performance index of these controllers for unit step input.

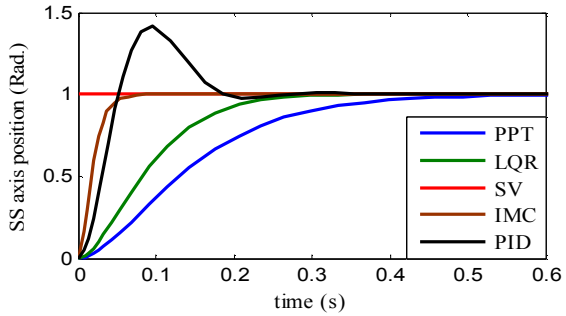

Fig. 12. Unit step response of all controller.

On the basis of fig.12 and table 4, the PPT, IMC and LQR has got negligible maximum overshoot (OS) and steady state error (Ess). The rise time (RT) and settling time (ST) for IMC is least in comparison to PPT, LQR and PID controllers. Hence IMC gives better performance result for nominal value of *K* (0.5) in comparison with other designed controllers i.e. PPT, LQR and PID etc. Subsequently relative efficacy of controllers is judged under parametric uncertainties.

Table 4. Performance indexs of controllers for unit step input.

Controller	ST(s)	RT(s)	OS (%)	Ess (%)
PID (ZN)	0.175	0.0525	41.62	0.0
PPT	0.42	0.263	0.0	0.0
LQR	0.25	0.16	0.0	0.0
IMC (μ=0.01)	0.055	0.034	0.0	0.0

Unit step response of SS axis position with PID, PPT, LQR, and IMC are shown in fig.13 to 16 under parametric uncertainties for different value of K for robust and optimal analysis. Using these figures the comprehensive table 5 is accomplished for robust and optimal analysis of designed controllers.

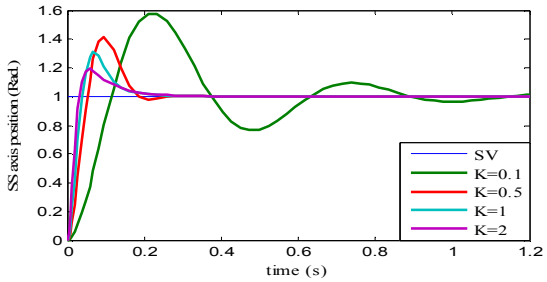

Fig. 13. Response with PID controller for different value of K.

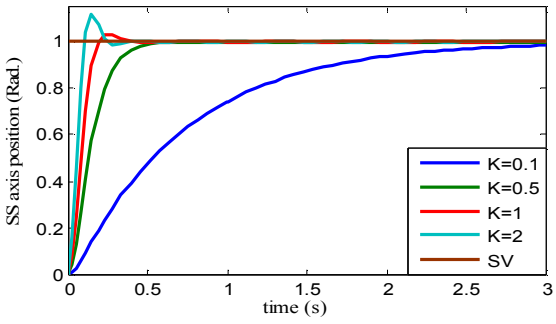

Fig. 14. Response with PPT for different value of K.

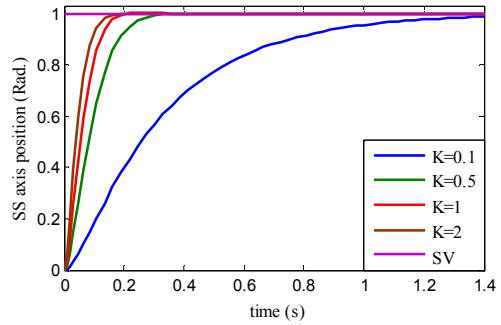

Fig. 15. Response with LQR for different value of K.

In table 5 the values of ST, RT, OS and Ess for PID, PPT, LQR and IMC are presented from the step response of fig. 13 to 16 respectively under parametric uncertainties for different values of K. Comparing the step response characteristics of sun seeker system using different controllers it is seen that the PID though is slightly faster in response than PPT yet highly oscillatory due to very large OS. It is also observed that under parametric uncertainties if the overshoot is condoned, IMC outperforms all other controllers as far as speed of response is concerned. It is obvious from table 5 that the rise time band for K varying from 2 to 0.1 is 0.0125 sec to 0.2 sec for IMC controller whereas for LQR is 0.08 sec to 0.684 sec. Similarly the settling time band under same range of variation of K for IMC is 0.038 sec to 0.35 sec whereas for LQR is from 0.13 sec to 1.1 sec.

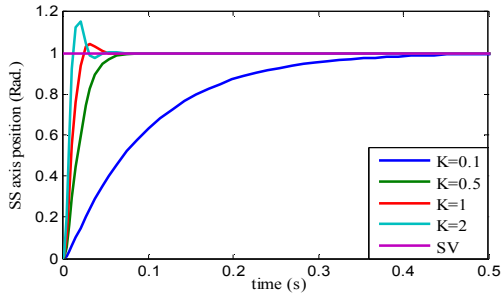

Fig. 16. Response with IMC for different value of K.

Table 5. Performance Index of Controllers for different K.

Controller	Gain(K)	ST (s)	RT (s)	OS(%)	Ess (%)
PID	0.1	1.05	0.1148	57.84	1.14
	0.5	0.175	0.0525	41.62	0.0
	1	0.17	0.0397	31	0.0
	2	0.168	0.033	19.2	0.0
PPT	0.1	2.75	1.549	0.0	0.0
	0.5	0.42	0.263	0.0	0.0
	1	0.295	0.1936	3.1	0.0
	2	0.22	0.1023	12.1	0.0
LQR	0.1	1.1	0.684	0.0	0.0
	0.5	0.25	0.16	0.0	0.0
	1	0.16	0.104	0.2	0.0
	2	0.13	0.08	0.1	0.0
IMC	0.1	0.35	0.2	0.0	0.0
	0.5	0.055	0.034	0.0	0.0
	1	0.04	0.025	4.32	0.0
	2	0.038	0.0125	15.25	0.0

Similarly taking the rise-time band and settling-time band for PID and PPT under same parametric uncertainties, and comparing it with LQR and IMC, following findings and inferences are drawn. First it is observed that under parametric uncertainties, IMC controller gives robust performance. Similarly if the efficacy of controllers are investigated in terms of overshoots and oscillations it is observed that the OS for PID is maximum (57.84%) followed by IMC and PPT respectively. The most startling fact is that the OS for LQR is negligible. Hence the response corresponding to LQR is less oscillatory and exhibits less maximum overshoot. Hence with regard to overshoot and oscillation, LQR outperforms all the other controllers. OS in the system has some implication with the energy consumption. The presence of overshoot is akin to the uneven road where vehicle would consume more fuel hence this way optimal controller mitigates the overshoot and gives less oscillatory response which in turn consumes less energy. In context with the present SSS, high oscillation and OS implies the nonalignment of vehicle axis with solar axis and hence the presence of error signal which will put the respective controller in action till these spurious things dies out. In doing so heavy energy loss takes place and by using LQR we can optimize the energy consumption to a great extent because OS is negligible.

7. CONCLUSION

In this paper the sun seeker system (SSS) which consists of Photo voltaic (PV) cells are mounted on space vehicle to provide the required electrical energy to it. The objective of sun seeker system is to manoeuvre its own attitude continuously so as to extract maximum possible current from PV cell. In this paper the design of robust and optimal controllers are presented to precisely control the sun seeker axis position of sun seeker so that maximum possible current may be supplied by the PV cells. The results of proposed controllers, IMC for robust and LQR for optimal control under perturbed conditions are compared with classical PID controller and PPT. It is observed that if the negligible overshoot is condoned, IMC outperforms other controllers with regard to transient and steady state response. Conversely if overshoot feature is not condoned then LQR gives overall best performance because it completely decimates the OS and makes the design less oscillatory. So even for the other processes where perturbation exists, LQR controller will be the preferred choice. In a similar way for the system where there is big scope of parametric variations, system will be sluggish if controller does not take swift action. Hence for these systems IMC displays the desired robust feature. So even when the space vehicle encounters the erratic situation, IMC and LQR in tandem, may work as a panacea. This kind of research work may encourage for maximum use of renewable energy sources in every walk of life which otherwise is sparingly used all over the world.

APPENDIX A

A general control model for the sun seeker system is presented below. The LQ optimal control model, PID and IMC controllers can be derived as special cases of the model. Let $\theta_r(t)$ be the sun ray's angle relative to a fixed reference and let $\theta_m(t)$ be the angle turned by the dc motor. Let $\theta_o(t)$ be the angle turned by the sensor (PV) plates relative to the

fixed reference. The aim of the sun seeker system is to make $\theta_o(t) = \theta_r(t)$ i.e. $\alpha(t) = \theta_r(t) - \theta_o(t) = 0$. If $\alpha(t) \neq 0$, then the motor receives an input current equal to $i(t) = g(\alpha(t)) = g(\theta_r(t) - \theta_o(t))$. The angle turned by the motor $\theta_m(t)$ is proportional to $\theta_o(t)$ i.e. $\theta_o(t) = \gamma.\theta_m(t)$, where γ is a constant, determined by the gear system. So the dynamics of the servo motor is given by

$$J\ddot{\theta}_m(t) + B\dot{\theta}_m(t) = kg(\theta_r(t) - \gamma.\theta_m(t)).sin(\theta_m(t)) \quad (40)$$

The function g satisfies $g(0) = 0$ and

$g(x) > 0$ if $0 < x < \frac{\pi}{2}$

$g(x) < 0$ if $-\pi/2 < x < 0$

This guaranties that $\theta_m(t)$ increases if the error

$$\alpha(t) = \theta_r(t) - \theta_o(t) = \theta_r(t) - \gamma.\theta_m(t) > 0$$

and decreases if

$$\alpha(t) = \theta_r(t) - \theta_o(t) = \theta_r(t) - \gamma.\theta_m(t) < 0.$$

By changing the function g we achieve any desired performance. Optimal control will be used if we desire to spend minimum energy in achieving alignment.

Suppose we wish alignment at time T, then the current through the motor which is $g(\alpha(t)) = g(\theta_r(t) - \gamma.\theta_m(t))$ may be modified to $g(\theta_r(t) - \gamma.\theta_m(t), u(t))$ where $u(t)$ is a control input and the energy spent is proportional to

$$E = \int_0^T g^2\big(\theta_r(t) - \gamma.\theta_m(t), u(t)\big)dt \quad (41)$$

g is now a new function of two variable. This energy must be minimized subject to the final point constraint.

$\gamma.\theta_m(T) = .\theta_r(T)$, and the equation of motion

$$\dot{\theta}_m(t) = \omega_m(t), \quad (42)$$

$$J\dot{\omega}_m(t) + B\omega_m(t) = kg(\theta_r(t) - \gamma.\theta_m(t), u(t)).sin(\theta_m(t) \;; 0 \leq t \leq T \quad (43)$$

Therefore the functional to be minimized after incorporating Lagrange multipliers $\lambda_1(t)$, $\lambda_2(t)$ and $\lambda_3(t)$.

$$\begin{aligned} &E\big(\theta_m(\cdot), u(\cdot), \lambda_1(\cdot), \lambda_2(\cdot), \lambda_3(\cdot)\big) \\ &= \int_0^T g^2\big(\theta_r(t) - \gamma.\theta_m(t), u(t)\big)dt \\ &+ \int_0^T \lambda_1(t)\left(\dot{\theta}_m(t) - \omega_m(t)\right)dt \\ &+ \int_0^T \lambda_2(t)\Big(J\dot{\omega}_m(t) + B\omega_m(t) \\ &\qquad - kg\big(\theta_r(t) - \gamma.\theta_m(t), u(t)\big)\Big)dt \\ &+ \lambda_3(\gamma.\theta_m(T) - \theta_r(T)) \end{aligned} \quad (44)$$

APPENDIX B

Derivation of Matrix Riccati Equation for a Process of Finite Duration

In order to apply optimal control law, the matrix $P(t)$ is required which is normally obtained by solving the matrix Riccati equation. Hence here the general matrix Riccati equation for linear time variant system has been derived from the already derived equations (21) through (34). Next the same for time invariant system are derived with some additional conditions (Gopal, 2009; Kirk, 1970).

Clubbing of (21), (32) and (33) we get

$$\dot{x} = A(t)x(t) - B(t)R^{-1}B^T(t)P(t)x(t) \quad (45)$$

Also from (31)

$$\dot{\lambda}(t) = \dot{P}(t)x(t) + P(t)\dot{x}(t) \quad (46)$$

And from (28)

$$\dot{\lambda}(t) = -Q(t)x(t) - A^T(t)P(t)x(t) \quad (47)$$

Combining (46) and (47)

$$\dot{P}(t)x(t) + P(t)\dot{x}(t) = -Q(t)x(t) - A^T(t)P(t)x(t) \quad (48)$$

But from (21), we get $\dot{x} = A(t)x(t) + B(t)u(t)$ which when clubbed with (48) gives

$$\begin{aligned} &\big[\dot{P}(t) + P(t)A(t) + A^T(t)P(t) - \\ &P(t)B(t)R^{-1}(t)B^T(t)P(t) + Q(t)]x(t) = 0 \end{aligned} \quad (49)$$

Since this must hold for all non-zero $x(t)$, the term pre-multiplying $x(t)$ must be zero. Thus the matrix $P(t)$, which is a $n \times n$ symmetric matrix, must satisfy the matrix Riccati equation

$$\begin{aligned} &-\dot{P}(t) = P(t)A(t) + A^T(t)P(t) \\ &-P(t)B(t)R^{-1}(t)B^T(t)P(t) + Q(t) \end{aligned} \quad (50)$$

Equation (50) is known as matrix Riccati equation. Since P is an $n \times n$ matrix, Eq. (50) is a system of n^2 first order differential equation. Actually, it can be shown that P is

symmetric; hence, not n^2 but $n(n+1)/2$ first order differential equation must be solved. These equations can be integrated numerically by using a digital computer. The integration is started at $t = t_f$ and proceeds backward in time at $= t_0$; matrix $P(t)$ is stored, and the feedback gain matrix $k(t)$ is determined from (34).

Kalman's Modified Matrix Riccati Equation for a Process of Infinite Duration

In previous section matrix Riccati equation has been derived for finite duration. Here in this section the Kalman's modified matrix Riccati equation has been considered for an interval of infinite duration. The situation wherein the process is to be controlled for an interval of infinite duration merits special attention. Kalman (Kirk, 1970) has modified the original matrix Riccati equation by considering the following changes in the parameters of performance measure:

The plant is completely controllable

$H = 0$, and

Matrix A, B, R, and Q are constant matrices

Kalman has shown that if the above hypotheses are satisfied then the matrix $P(t)$ will become a constant matrix P for an interval of infinite duration i.e. if $t_f \to \infty$. The engineering

implication of this result is very important. If the above hypotheses are satisfied, then the optimal control law for an infinite duration process is stationary. This means that the implementation of the optimal controller in this case also is as usual except that $k(t)$ is constant. From a practical perspective, it may be feasible to use fixed control law even for process of finite duration. Taking reference of many practical examples of process of finite duration where objective of the controller is to regulate the value of different states be zero level within stipulated final time t_f, it is observed that the states reach the zero level well before the stipulated time. This means that constant matrix P can be used without significant performance degradation. Hence the designer needs to compare system performance using the steady state gains with performance using time varying optimal gains to decide which should be implemented. To determine the P matrix for an infinite time process, the Riccati equation is integrated backward in time until a steady state solution is obtained or solving the nonlinear algebraic equations

$$0 = -PA - A^T P + PBR^{-1}B^T P - Q \tag{51}$$

obtained by setting $\dot{P}(t) = 0$ in Eq. (50). Equation (51) is Kalman's modified matrix Riccati equation for an interval of infinite duration.

REFERENCES

Amuthan, N., Mohan, R., Kumar, N. S. and Suganya, T. (2009). Dynamic speed response of internal model controller for time delay plant with dither injection. *International Journal of Recent Trends in Engineering*, 2(7), 16-18.

Borrelli, F. and Keviczky, T. (2008). Distributed LQR design for identical dynamically decoupled systems. *IEEE Transactions on Automatic Control*, 53(8), 1901-1912.

Canale, M., Fagiano, L., Ferrara, A. and Vecchio, C. (2009). Comparing internal model control and sliding-mode approaches for vehicle yaw control. *IEEE Transactions on Intelligent Transportation Systems*. 10(1), 31-41.

Ehsani, M., Gao, Y., and Emadi, A. (2011). *Modern electric hybrid electric and fuel cell vehicles*. Second Edition, CRC Press, New York, USA.

Gevorkian, P. (2011). *Large scale solar power system design*. McGraw Hill Companies, New York, USA.

Gollman, L., Kern, D. and Maurer, H. (2009). Optimal control problems with delays in state and control variables subject to mixed control-state constraints. *Journal of Optimal Control Applications and Methods*, 30, 341-365.

Gopal, M. (2009). *Digital control and state variable methods conventional and intelligent control system*. Tata Mcgraw Hill Education Pte. Ltd., Third Reprint.

Hamedmouna, B. and Lassad, S. (2007). Internal model controller of an ANN speed sensor less controlled induction motor drives. *Journal of Applied Science*, 7, 1456-1466.

Harnefors, L. and Nee, H.P. (1998). Model-based current control of AC machines using the internal model control method. *IEEE Transactions on Industry Applications*, 34(1), 133-141.

Husain, I. (2011). *Electric and hybrid vehicles, design fundamentals*. Second Edition, CRC Press, Taylor and Francis Group, New York, USA.

Kakilli, A., Oguz, Y. and Alik, H.C. (2009). The modelling of electric power systems on the state space and controlling of optimal LQR load frequency. *Journal of Electrical & Electronics Engineering,* 9(2), 977-982.

Kiencke, U. and Nielsen, L. (2007). *Automotive control system for engine, driveline and vehicle*. Springer (India) Pte. Ltd, Second Edition, first Indian reprint.

Kirk, D.E. (1970). *Optimal control theory, an introduction*. Prentice Hall, Englewood cliffs, New Jersey.

Kuo, B.C. and Golnaraghi, F. (2003). *Automatic control system*. John Wiley and Sons (Asia) Pte Ltd, Eighth Edition.

Li, H.X. and Deng, H. (2006). An approximate internal model-based neural control for unknown nonlinear discrete processes. *IEEE Transactions on Neural Networks*, 17(3), 659-670.

Malan, S., Milanesen, M., Regruto, Y.D. and Taragna, M. (2004). Robust control from data via uncertainty model sets identification. *International Journal of Robust and Nonlinear Contro*l, 14, 945–957.

Mi, C., Lin, H. and Zhang, Y. (2005). Iterative learning control of antilock braking of electric and hybrid vehicles. *IEEE Transactions on Vehicular Technology*, 54(2), 486-494.

Mikles, J. and Fikar, M. (2007). *Process modelling, identification and control*. Springer Berlin Heidelberg New York, USA.

Oner, K.T., Cetinsoy, E., Sirimoglu, E., Hancer, C., Ayken, T. and Unel, M. (2009). LQR and SMC stabilization of a new unmanned aerial vehicle. *World Academy of Science, Engineering and Technology* 58, 554-559.

Peterson, I.R. (2009). Robust H^{∞} control of an uncertain system via a strict bounded real output feedback controller. *Journal of Optimal Control Application and Methods*, 30, 247-266.

Skogestad, S. and Postlethwaite, I. (2001). *Multivariable feedback control analysis and design.* John Wiley & Sons, Second Edition.

Yadav, A.K., Gaur P., Jha, S.K., Gupta, J.R.P., and Mittal A.P. (2011). Optimal speed control of hybrid electric vehicles. *Journal of Power Electronics*, 11(4), 393-400.

Yadav, A.K. and Gaur, P. (2013). Comparative analysis of modern control and AI-based control for maintaining constant ambient temperature. *World Review of Science, Technology and Sustainable Development*, 10(1/2/3), 56–77.